チニン比と関連するタンパク質を解析した結果、これまでに 2 型糖尿病や糖尿病腎症との関連が報告されていないタンパク質 1 種を含む 6 タンパク質の同定に成功した。

B. 研究方法

1. 解析対象検体

独立行政法人国立国際医療研究センター病院 糖尿病・代謝・内分泌科に通院する微量アルブミン尿を呈していない 2 型糖尿病患者(T2DM, 男性 4 名、女性 2 名)、腎症病期 3 期の糖尿病腎症患者(DN3, 男性 4 名、女性 2 名)から採取した随時尿を探索用検体とした(表 1)。検証用検体として、T2DM(男性 8 名、女性 10 名)、DN3(男性 10 名、女性 5 名)に加え、腎症病期 2 期の糖尿病腎症患者(DN2, 男性 10 名、女性 10 名)から採取した随時尿を解析対象とした。2 型糖尿病の診断は日本糖尿病学会の「糖尿病分類と診断基準に関する委員会報告」に基づいて行った。また、独立行政法人国立国際医療研究センター病院人間ドックに来院した男性 17 名、女性 10 名より随時尿を採取し、検証用検体における健常者対照群(H)とした。これら検証用検体の臨床情報を表 2 に示す。

本研究の実施に当たり、事前に独立行政法人国立国際医療研究センター倫理員会にて研究遂行内容の承認を受けた。被験者に対しては、研究趣旨や利益、不利益、権利などを十分に説明し、インフォームドコンセントが得られた被験者からのみ検体を採取した。

Table 1: Characteristics of individuals examined in this study

	Type 2 diabetes mellitus (T2DM) (M4, F2)		Diabetic nephropathy with macroalbuminuria (DN3) (M4, F2)		
	Mean	SD	Mean	SD	*P* value*
Age (year)	60.2	4.8	63.5	1.9	0.10
T2DM Duration (year)	12.3	5.8	14.5	10.8	0.63
BMI (kg/m^2)	24.7	4.5	25.6	5.7	0.87
SBP (mmHg)	121.2	14.1	137.7	13.6	0.10
DBP (mmHg)	69.6	11.5	72.2	15.8	0.86
AST (IU/l)	26.6	12.5	22.3	3.2	0.65
ALT (IU/l)	28.2	16.4	21.0	7.1	0.38
γ-GTP (IU/l)	40.0	24.5	21.5	15.4	0.10
TC (mg/dL)	160.2	21.3	182.3	29.5	0.26
HDL (mg/dL)	43.5	7.5	48.5	10.8	0.52
TG (mg/dL)	88.8	14.9	141.0	91.1	0.47
Fasting glucose (mg/dL)	131.7	28.2	126.8	36.5	0.87
HbA1c (%)	7.6	0.7	6.7	0.9	0.09
Creatinin (mg/dL)	0.6	0.1	0.9	0.3	0.05
Uric acid (mg/dL)	6.6	4.7	5.8	0.9	0.67
eGFR (mL/minute per 1.73 m^2)	95.5	19.4	66.6	22.1	0.02
Albumin Creatinin ratio (mg/g Cre)	9.9	4.6	1097.5	757.2	0.004

*Mann-Whitney U test

Table 2. Characteristics of healthy control, type 2 diabetic, and diabetic nephropathy subjects for the validation study.

	Healthy	T2DM	Diabetic nephropathy with microalbuminuria (DN2)	Diabetic nephropathy with macroalbuminuria (DN3)	*p*-values*
Age (year)	57.7 ± 7.8	62.3 ± 4.1	61.0 ± 6.5	61.1 ± 7.2	0.26
Sex (male/female)	17/10	8/10	10/10	10/5	0.51
T2DM Duration (year)	-	16.7 ± 7.8	15.4 ± 8.8	14.9 ± 9.8	0.57
BMI (kg/m^2)	22.2 ± 3.0	25.0 ± 4.1	25.9 ± 4.8	27.1 ± 8.6	0.03
SBP (mmHg)	117.1 ± 10.0	121.4 ± 13.6	128.9 ± 14.8	131.6 ± 9.4	0.002
DBP (mmHg)	74.1 ± 9.3	69.6 ± 10.4	72.4 ± 9.6	68.8 ± 12.2	0.44
AST (IU/l)	24.0 ± 6.1	22.5 ± 8.7	23.9 ± 9.1	29.6 ± 13.3	0.25
ALT (IU/l)	22.3 ± 8.6	26.6 ± 16.4	27.7 ± 19.3	30.2 ± 18.1	0.81
γ-GTP (IU/l)	30.8 ± 15.4	33.1 ± 18.5	35.7 ± 32.3	146.3 ± 365.3	0.28
TC (mg/dL)	192.9 ± 18.4	195.8 ± 33.6	180.9 ± 16.4	172.4 ± 33.4	0.048
HDL (mg/dL)	65.7 ± 17.0	57.5 ± 16.5	51.2 ± 10.2	54.7 ± 20.3	0.045
TG (mg/dL)	86.4 ± 30.6	114.1 ± 60.2	111.3 ± 43.6	167.7 ± 134.7	0.12
Fasting glucose (mg/dL)	91.8 ± 6.4	142.7 ± 50.7	147.1 ± 40.8	168.6 ± 105.3	<0.001
HbA1c (%)	5.2 ± 0.3	7.0 ± 1.0	7.6 ± 1.1	7.1 ± 1.3	<0.001
Creatinin (mg/dL)	0.7 ± 0.1	0.7 ± 0.2	0.8 ± 0.3	1.2 ± 0.9	0.20
Uric acid (mg/dL)	5.3 ± 1.2	4.7 ± 1.0	5.1 ± 1.4	5.9 ± 1.5	0.09
eGFR (mL/minute per 1.73 m^2)	84.9 ± 19.2	76.2 ± 18.6	70.9 ± 18.8	64.3 ± 34.3	0.05
Albumin Creatinin ratio (mg/g Cre)	6.1 ± 3.7	10.8 ± 6.4	77.9 ± 50.9	1581.7 ± 2198.9	<0.001

*Kruskal-Wallis test

2. 検体の分離と精製

患者より採取した随時尿検体は3000×*g*, 10分, 4℃で遠心分離を行い、不純物を取り除いたのち速やかに凍結し解析に用いるまで-80℃にて保管した。各群の検体は、3 kDa cut offのAmicon Ultrafreeの限外ろ過で脱塩と濃縮を行った後にAlbmin & IgG Drpletion SpinTrap (GE Healthcare) にて尿中多量タンパク質を除去した。再び、3 kDa cut offのAmicon Ultrafreeの限外ろ過で脱塩と濃縮を行い乾固した後に12 mM sodium deoxycholate (SDC)/12 mM sodium N-lauroylarcosinate (SLS)にて溶解し、95℃5分の変性、ならびに37℃にてLys-C、トリプシンによる酵素消化を行った。さらにDTTを加え37℃、1時間、ヨードアセトアミドで暗室1時間反応させ還元アルキル化を行った。界面活性剤の除去はPhase Transfer Surfactant法(J. Proteome Res., 2008, 7: 731–740)にて行い、Mono Spin C18 (GE Healthcare)にて精製後、得られたペプチドをLC-MS解析用サンプルとした。

3. LC-MS測定、ならびに非標識定量解析

断片化された尿ペプチドサンプルの測定は、QSTAR Elite system(Applied Biosystems)にPAL/Paradigm LC system(ARM)を接続した

装置を用いた。カラムは 0.3 × 5 mm L-trap column と 0.1 × 150 mm L-column（財団法人化学物質評価研究機構）を用いて、流速 300 nL/min 、A 溶媒（2% ACN and 0.1%FA）、B 溶媒（90% ACN and 0.1%FA）で 175 min 間（グラジエント 5–30% B, 20 min); 30–95% B, 1 min; 95% B, 3 min; 95–5% B, 1 min; 5% B, 10 min）測定を行った。質量分析器のピーク検出と正規化、定量化は 2DICAL ソフトウェア（三井情報株式会社）を用いた。ピークのターゲットは、保持時間（RT）10-100min、ピークの最大強度 30 以上、P 値 0.05 未満のピークを選出した。選出されたピークは T2DM と DN3 で強度比に差のあるピークを目視により選別し LC-MS/MS 測定を行った。

4. LC-MS/MS 測定

タンパク質同定に当たっては 2DICAL のピーク情報をもとに m/z と RT を include list に設定し LC-MS/SM 測定を行った。得られたターゲットピーク情報から SwissProt データベースと Mascot ソフトウェア（Matrix science）を用いてタンパク質同定を行い、2DICAL 上のピークに対応させた。Mascot ソフトウェアの検索パラメーターには、MS の許容誤差 0.1Da、MS/MS の許容誤差 0.1Da 、固定修飾 carbamidomethyl (C) 、可変修飾 acetyl (N-term)、deamidated (NQ)、oxidation (M)、価数 2+, 3+, 4+を用いた。T2DM 群と DN3 群の発現差異を認めるピークの選定には、DN3 群のピーク定量値が T2DM 群のピーク定量値に対して 3 倍以上、RATIO P 値＜0.05、Mann-Whitney U 検定による P 値＜0.05、Mascot Score≧20 の指標を用いた。

5. MRM 定量解析

H群、T2DM群、DN2群、DN3群から構成される尿検体80サンプルを用いて、非標識定量解析にて同定された発現変動タンパク質群の検証を行った。バイオマーカー候補タンパク質群の相対タンパク質濃度はMRM法により算出した。MRM transitionには、Mascotデータからペプチドの親イオンのm/zをQ1とし、フラグメントイオンのm/zをQ3とし設定した。また、Enhanced Product Ion（EPI）-MS/MSにてタンパク質の同定を行い、設定したMRM transitionにより標的ペプチド配列が同定されることを確認した。なお、EPI-MS/MSにて同定出来ないペプチド配列に関しては、合成ペプチドを用い分析用試料と同時測定してMRM取得ピーク、溶出時間が一致することを確認した。尿検体の酵素消化産物に内部標準ペプチドとして安定同位体元素標識ペプチド30fmolを加え、分析用試料としてMRM測定を行った。MRM定量解析は、4000QTrap（ABSciex）にLC800 HPLC system（GL）を接続したシステムを用いて行った。カラムはACQUITY UPLC BET C18 カラム（Waters）を用いて流速100nl/min, 0%-30% Bで90分直線濃度勾配にて溶出した。Multiquant Software 2.0（AB Sciex）にてMRM測定により

得られた各ペプチドのシグナル面積値を内部標準物質より得られたペプチドのシグナル面積値で補正し、相対タンパク質濃度を算出した。

6. 統計解析

各測定値は平均値±標準偏差で示した。2群間の有意差検定はMann-Whitney U testにて、多群間の有意差についてはKruskal-Wallis検定にて行い、$p<0.05$を有意とした。重回帰分析、receiver-operating characteristic（ROC）解析はIBM SPSS statistics 20ソフトウェアにて行った。

C. 研究結果

T2DMおよびDN3の各6名ずつの検体から尿中タンパク質を精製しプロテアーゼ消化を行った。2DICALを用いた解析により合計3,334ピークが得られ、そのうち保持時間（RT）10-100min、ピークの最大強度30以上、P値0.05未満のピークは234であった。図1に全てのすべてのMSピークの2次元ゲル画像を示す。m/zをX軸、RTをY軸とし、最大強度30以上あった234ピークを黄色で強調した。選出された234ピークのなかで、DN1とDN3で強度比に有意な差のある107ピークを目視により選別した（図2）。これら107ピークのLC-MS/MS測定により、T2DM群に対してDN3群で3倍以上の有意な発現変動を示すタンパク質が30種類同定された（表3）。それら30種類のタンパク質のなかで、メチオニンの酸化もしくは、miss cleavageの

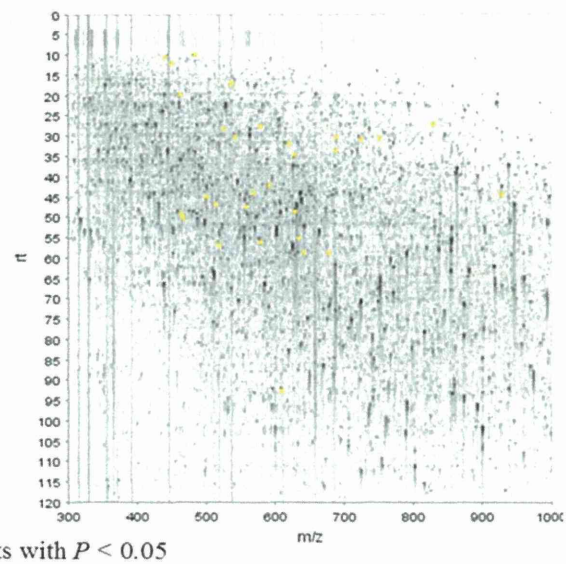

Figure 1. Two-dimensional display of all MS peaks. The 107 MS peaks whose mean intensities significantly differed between DN1 and DN3 ($P < 0.05$, Welch's t-test) are highlighted in red. RT: retention time.

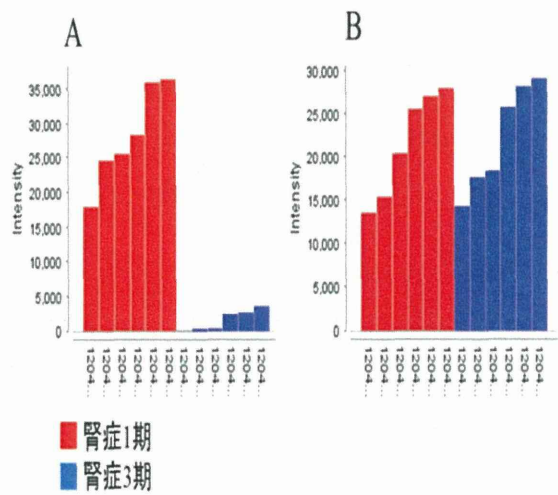

Figure 2. A, B: MS peaks of peak in duplicate LC-MS runs (6 with DN3 (left) and 6 with DN1(right)) aligned along LC RT. Columns represent the mean intensities of triplicate runs.

Table 3. Summary of protein identification by tandem mass spectrometry

ID	*m/z*	RT	Charge	T2DM (mean±SD)	DN3 (mean±SD)	*P* values*	Mascot score	Peptide sequence	Protein description
50	632.9	55.2	2	51±36	4778±6415	3.2E-03	92.7	SGLSTGWTQLSK	Alpha-1B-glycoprotein
141	608.4	92.5	2	36±34	2033±3574	1.6E-03	84.7	ITLLSALVETR	Alpha-1-antichymotrypsin
1481	556.8	47.4	2	21±12	1148±1749	3.9E-04	76.9	SDVVYTDWK	Alpha-1-acid glycoprotein 1
143	676.9	58.6	2	5±3	3289±2267	3.9E-04	72.6	AREDIFMETLK	Zinc-alpha-2-glycoprotein
202	688.3	30.2	2	52±87	2442±2893	1.4E-02	67.4	TFTCTAAYPESK	Ig alpha-1 chain C region
65	567.3	44.0	2	1842±3798	38±17	8.2E-04	65.2	VFMYLSDSR	Uromodulin
514	626.8	34.5	2	13±7	822±737	2.9E-02	64.3	MFTTAPDQVDK	Ceruloplasmin
231	577.3	56.1	2	3299±2412	68±57	1.2E-03	63.8	ALSIGFETCR	CD44 antigen
3130	524.3	28.1	2	11±10	59±52	1.2E-03	62.5	CNSLSTLEK	Lysosome-associated membrane glycoprotein 2
12	461.7	19.7	2	245±415	12965±9338	2.3E-03	59.3	FLENEDR	Alpha-1-antitrypsin
1	499.3	44.9	2	351±794	23692±12235	1.6E-03	55.1	ASYLDCIR	Serotransferrin
783	540.8	30.1	2	4±1	478±371	4.3E-03	54.4	TLSDYNIQK	Ubiquitin-40S ribosomal protein S27a
293	750.4	30.5	1	38±66	1968±1452	3.9E-04	45.4	FIEDVK	Obscurin
253	482.8	9.8	2	19±20	1482±1730	2.3E-03	44.6	HHGPTITAK	Protein AMBP
1228	723.4	30.7	1	6±3	146±214	5.7E-04	36.6	EGENFK	Tetratricopeptide repeat protein 9A
435	590.8	42.1	2	29±25	1883±1703	1.2E-03	36.3	WLDGTSPDYK	Collectin-12
209	448.8	11.9	2	5±4	84±50	3.9E-04	32.1	HLELKEK	N-alpha-acetyltransferase 10
358	561.3	38.4	2	17±13	168±330	4.3E-03	22.8	FVDPNTQEK	Epiplakin
77	512.8	46.7	2	2369±5553	75±79	1.7E-01	36.6	MALEVGDYK	Cadherin-1
410	707.4	27.1	1	33±85	1557±1751	1.6E-03	26.9	PGLYNK	Dynein heavy chain 17
97	686.5	33.7	1	53±55	1543±133	3.9E-04	53.9	AVDIVK	Poly [ADP-ribose] polymerase 14
134	474.3	33.7	1	93±105	2766±1967	3.9E-04	26.0	GGPVK	Probable E3 ubiquitin-protein ligase TRIP12
59	640.4	58.5	2	33±28	8903±9672	5.7E-04	31.2	NLLEQIVLPLK	Metastasis-associated in colon cancer protein 1
825	516.8	56.7	2	9±8	605±640	8.2E-04	30.0	AIPVTQYLK	Afamin
870	577.3	27.4	1	7±5	472±882	3.9E-04	29.2	TDITK	NADPH:adrenodoxin oxidoreductase, mitochondrial
504	465.8	50.1	2	427±801	12±15	3.9E-04	28.1	FSSQFVSK	SUN domain-containing protein 1
792	462.2	49.1	2	931±818	47±45	8.2E-04	28.1	VSCVTPNF	WAP four-disulfide core domain protein 2
386	618.8	31.9	2	1019±1597	14±7	3.9E-04	26.9	VAGPWGPGLVQR	Abhydrolase domain-containing protein 4
210	627.5	48.6	1	15±19	1806±2718	7.0E-04	26.2	IIILR	Dynein heavy chain 12, axonemal
437	927.5	44.5	1	11±4	961±2107	7.0E-04	22.8	SGLTEHQR	Zinc finger protein 613

RT, retention time; T2DM, type 2 diabetes mellitus without nephropathy; DN3, diabetic nephropathy with macroalbuminuria. *: Mann-Whitney U test.

存在が推定された5種類のタンパク質を除く25種類のタンパク質(発現上昇タンパク質:20、発現減少タンパク質:5)について、一斉分析が可能な定量解析法であるMRM法を用いて尿中相対タンパク質濃度を測定した。MRM法のtransition設定は以下に従って行った。すなわち、Mascotデータからペプチドの親イオンのm/zをQ1とし、フラグメントイオンのm/zをQ3の値とした111組のtransitionで測定した。EPI-MS/MS測定により、12種類の標的ペプチド配列が同定され、残り13種類のタンパク質については合成ペプチドを用いてMRM transitionの確認を行った。25種類のタンパク質を標的とするMRM transitionを用いて、T2DM群18名、DN3群15名の検体の尿中相対タンパク質濃度を測定した。25種類のタンパク質中19種類のタンパク質がH群、T2DM群、DN2群、DN3群間で有意な発現変動を示した。このうち非標識定量解析と同様の発現変動が検証されたタンパク質は16種類(発現上昇タンパク質:13、発現減少タンパク質:3)だった。

糖尿病腎症の早期尿中関連因子を絞り込む目的で、H群27名、DN2群20名におけ

る25蛋白質の尿中相対タンパク質濃度を追加測定し先のデータと併せて重回帰分析を行った。解析の結果、尿中アルブミン・クレアチニン比にafamin（β:0.33, $p=1.8\times10^{-7}$)、CD44 antigen（β:-0.17, $p=1.5\times10^{-3}$)、alpha-1-antitrypsin（β:0.21, $p=7.5\times10^{-5}$)、epiplakin（β:0.21, $p=4.9\times10^{-6}$)、Ig alpha-1 chain C region（β:0.15, $p=1.5\times10^{-3}$)、WAP four-disulfide core domain protein 2（β:-0.15, $p=6.4\times10^{-3}$)、alpha-1-acid glycoprotein 1（β:0.12, $p=0.027$)の7タンパク質が関連することが示された。早期腎症以降への進展を基準評価としたROC解析では、epiplakinを除くafamin（AUC:93.5%)、CD44 antigen（AUC:90.7%)、alpha-1-antitrypsin（AUC:81.4%)、Ig alpha-1 chain C region（AUC:75.2%)、WAP four-disulfide core domain protein 2（AUC:77.3%)、alpha-1-acid glycoprotein 1（AUC:87.6%)の6タンパク質が良好な診断能を示した。なお、腎機能評価に用いられるeGFRのROC曲線下面積は64.9%であり、本研究での検証集団における判定能はeGFRよりも上記6タンパク質の方が優れていた。

さらに上記6タンパク質に加えて性別、糖尿病罹病期間、BMI、収縮期血圧、トリグリセリド、空腹時血糖、HbA1c、eGFRを説明変数とした多重ロジスティック回帰分析を行った。早期腎症以降への進展に及ぼす因子として afamin（オッズ比:1.71; 95% CI:1.16-2.52; p＝0.007)、ならびにCD44 (オッズ比:0.98, 95% CI:0.96-0.99, p＝0.004)が選択された。Afamin と CD44のそれぞれのカットオフ値を用いることにより感度、特異度がいずれも100%を示し、

Table 4. Diagnostic discrimination between diabetic nephropathy patients (DN2 and DN3) and non-diabetic nephropathy subjects (H and T2DM).

Protein description	Cutoff value	Sensitivity, %	Specificity, %
Afamin	8.7	93.5	87.0
CD44 antigen	250.5	79.5	89.5
Alpha-1-antitrypsin	7.5	70.6	74.4
Epiplakin	3.3	71.4	64.3
Ig alpha-1 chain C region	16.6	67.6	75.0
WAP four-disulfide core domain protein 2	58.1	63.8	83.3
Alpha-1-acid glycoprotein 1	523.9	77.8	82.9
Afamin/CD44 antigen	8.7/250.5	100	100

本研究での検証集団をより正確に判定することが出来た(表 4)。

D. 考察

本研究で我々は非標識定量法を用いたプロテオーム解析により、T2DM 群、DN3 群の両群間で発現量に有意差を認める 30 種類のタンパク質を同定した。MRM 定量解析が可能であった 25 タンパク質を対象に T2DM 群、DN3 群の尿中タンパク質濃度を測定した結果、16 種類のタンパク質(発現上昇タンパク質:13、発現減少タンパク質:3)の発現変動が独立集団においても検証された。尿中アルブミン・クレアチニン比との関連が示された 7 タンパク質のうち、afamin は糖尿病、ならびに糖尿病性血管合併症に関する血清・尿プロテオーム解析にてその発現が上昇することが報告されているものの、その機能、意義についての報告はほとんど見られない。CD44 はヒアルロン酸を始めとする細胞外マトリックスと結合する接着分子であり、(1) リンパ球ホーミング、(2) リンパ球活性化、(3) 細胞-細胞間接着及び細胞-基質間接着、(4) 細胞運動、(5) 癌細胞増殖・転移などに深く関与していることが報告されている。CD44 の機能は発現量だけでなく、alternative splicing variant isoforms の発現、糖鎖付加やリン酸化等の翻訳後修飾によっても制御される。近年、CD44 は癌幹細胞マーカーとしての役割ばかりでなく、糖尿病腎症モデルである OVE26 マウス腎尿細管、ラット虚血腎モデルでの浸潤炎症細胞、腎移植後の急性拒絶反応時の尿においても発現上昇するとの報告があり、糖尿病腎症との関連も示唆されている。一方、WAP Four-Disulfide Core Domain Protein 2 (WFDC2) は WAP (Whey Acidic Protein) ファミリーに属する分子量約 25 kDa の分泌型糖タンパク質であり、HE4 (Human Epididymal Protein 4) とも呼ばれる。WFDC2/HE4 は, 正常な男女の生殖管上皮, 上気道, 唾液腺管, 胸部で発現しているほか, 遠位曲尿細管, 結腸, 子宮内膜でも可変的な発現が見られる。肺腺癌および肺嚢胞性線維症、子宮体癌、卵巣癌と WFDC2/HE4 発現との関連が報告されているものの、2 型糖尿病や糖尿病腎症との関連はこれまでのところ報告されていない。

本研究にて同定された尿タンパク質の発現変動と糖尿病腎症との関連をより大規模な集団において検証する必要があるものの、これらの尿中蛋白質は糖尿病腎症の発症・進展をより早期に検出する診断・予測マーカーとなる可能性がある。

E. 健康危険情報

該当事項なし

F. 研究発表

論文:

該当事項なし

学会発表:

なし

G. 知的財産権の出願・登録状況（予定を含む）

1.特許取得

出願準備中

2.実用新案登録

なし

3.その他

なし

Ⅲ. 研究成果の刊行に関する一覧表・別刷

雑誌

発表者氏名	論文タイトル名	発表誌名	巻号	ページ	出版年
Takahashi E, Okumura A, Unoki-Kubota H, Hirano H, Kasuga M, Kaburagi y.	Differential proteome analysis of serum proteins associated with the development of type 2 diabetes mellitus in the KK-A^y mouse model using the iTRAQ technique.	J Proteomics.	84	40-51	2013
Kimura K, Nakamura Y, Inaba Y, Matsumoto M, Kido Y, Asahara SI, Matsuda T, Watanabe H, Maeda A, Inagaki F, Mukai C, Takeda K, Akira S, Ota T, Nakabayashi H, Kaneko S, Kasuga M, Inoue H.	Histidine augments the suppression of hepatic glucose production by central insulin action.	Diabetes.	印刷中		2013
Asahara S, Shibutani Y, Teruyama K, Inoue HY, Kawada Y, Etoh H, Matsuda T, Kimura-Koyanagi M, Hashimoto N, Sakahara M, Fujimoto W, Takahashi H, Ueda S, Hosooka T, Satoh T, Inoue H, Matsumoto M, Aiba A, Kasuga M, Kido Y.	Ras-related C3 botulinum toxin substrate 1 (RAC1) regulates glucose-stimulated insulin secretion via modulation of F-actin.	Diabetologia.	56	1088-97	2013
Takahashi M, Inomata S, Okimura Y, Iguchi G, Fukuoka H, Miyake K, Koga D, Akamatsu S, Kasuga M, Takahashi Y.	Decreased serum chemerin levels in male Japanese patients with type 2 diabetes: sex dimorphism.	Endocr J.	60	37-44	2013
Kawano Y, Nakae J, Watanabe N, Fujisaka S, Iskandar K, Sekioka R, Hayashi Y, Tobe K, Kasuga M, Noda T, Yoshimura A, Onodera M, Itoh H.	Loss of Pdk1-Foxo1 signaling in myeloid cells predisposes to adipose tissue inflammation and insulin resistance.	Diabetes	61	1935-48	2012

発表者氏名	論文タイトル名	発表誌名	巻号	ページ	出版年
Imamura M, Maeda S, Yamauchi T, Hara K, Yasuda K, Morizono T, Takahashi A, Horikoshi M, Nakamura M, Fujita H, Tsunoda T, Kubo M, Watada H, Maegawa H, Okada-Iwabu M, Iwabu M, Shojima N, Ohshige T, Omori S, Iwata M, Hirose H, Kaku K, Ito C, Tanaka Y, Tobe K, Kashiwagi A, Kawamori R, Kasuga M, Kamatani N; Diabetes Genetics Replication and Meta-analysis (DIAGRAM) Consortium, Nakamura Y, Kadowaki T.	A single-nucleotide polymorphism in ANK1 is associated with susceptibility to type 2 diabetes in Japanese populations.	Hum Mol Genet.	21	3042-9	2012
Sakai M, Matsumoto M, Tujimura T, Yongheng C, Noguchi T, Inagaki K, Inoue H, Hosooka T, Takazawa K, Kido Y, Yasuda K, Hiramatsu R, Matsuki Y, Kasuga M.	CITED2 links hormonal signaling to PGC-1α acetylation in the regulation of gluconeogenesis.	Nat Med.	18	612-7	2012
Hamasaki H, Yanai H, Mishima S, Mineyama T, Yamamoto-Honda R, Kakei M, Ezaki O, Noda m.	Correlations of non-exercise activity thermogenesis to metabolic parameters in Japanese patients with type 2 diabetes.	Diabetol Metab Syndr.	27	26	2013
Okamoto M, Kishimoto M, Takahashi Y, Osame K, Noto H, Yamamoto-Honda R, Kajio H, Tokuhara M, Edamoto Y, Endo H, Igari T, Kubota K, Noda m.	A case of malignant insulinoma: successful control of glycemic fluctuation by replacing octreotide injections with octreotide LAR injections.	Endocr J.	印刷中		2013
Kurotani K, Nanri A, Goto A, Mizoue T, Noda m, Oba S, Kato M, Matsushita Y, Inoue M, Tsugane S; for the Japan Public Health Center-based Prospective Study Group.	Red meat consumption is associated with the risk of type 2 diabetes in men but not in women: a Japan Public Health Center-based Prospective Study.	Br J Nutr.	7	1-9	2013

発表者氏名	論文タイトル名	発表誌名	巻号	ページ	出版年
Matsushita Y, Nakagawa T, Yamamoto S, Kato T, Ouchi T, Kikuchi N, Takahashi Y, Yokoyama T, Mizoue T, Noda m.	Adiponectin and visceral fat associated with cardiovascular risk factors.	Obesity	印刷中		2013
Goto M, Morita A, Goto A, Deura K, Sasaki S, Aiba N, Shimbo T, Terauchi Y, Miyachi M, Noda m, Watanabe S; SCOP Study Group.	Reduction in adiposity, β-cell function, insulin sensitivity, and cardiovascular risk factors: a prospective study among Japanese with obesity.	PLoS One.	8	e57964	2013
Matsushita Y, Nakagawa T, Yamamoto S, Takahashi Y, Yokoyama T, Mizoue T, Noda m.	Effect of longitudinal changes in visceral fat area on incidence of metabolic risk factors: The hitachi health study.	Obesity	印刷中		2013
Noto H, Goto A, Tsujimoto T, Noda m.	Low-carbohydrate diets and all-cause mortality: a systematic review and meta-analysis of observational studies.	PLoS One.	8	e55030	2013
Sakane N, Kotani K, Takahashi K, Sano Y, Tsuzaki K, Okazaki K, Sato J, Suzuki S, Morita S, Izumi K, Kato M, Ishizuka N, Noda m, Kuzuya H.	Japan Diabetes Outcome Intervention Trial-1 (J-DOIT1), a nationwide cluster randomized trial of type 2 diabetes prevention by telephone-delivered lifestyle support for high-risk subjects detected at health checkups: rationale, design, and recruitment.	BMC Public Hlth.	13	81	2013
Goto A, Morita A, Goto M, Sasaki S, Miyachi M, Aiba N, Terauchi Y, Noda m, Watanabe S; Saku Cohort Study Group.	Associations of sex hormone-binding globulin and testosterone with diabetes among men and women (the Saku Diabetes study): a case control study.	Cardiovasc Diabetol.	11	130	2012

発表者氏名	論文タイトル名	発表誌名	巻号	ページ	出版年
Kishimoto M, Noda m.	Effect of the addition of sitagliptin and miglitol on insulin-treated type 2 diabetes.	Diabetes Ther.	3	11	2012
Kishimoto M, Noda m.	The Great East Japan Earthquake: Experiences and Suggestions for Survivors with Diabetes (perspective).	PLoS Curr.	4	e:4facf9d99b997	2012
Goto M, Morita A, Goto A, Sasaki S, Aiba N, Shimbo T, Terauchi Y, Miyachi M, Noda m, Watanabe S; SCOP Study Group.	Dietary glycemic index and glycemic load in relation to HbA1c in Japanese obese adults: a cross-sectional analysis of the Saku Control Obesity Program.	Nutr Metab	9	79	2012
Nanri A, Shimazu T, Takachi R, Ishihara J, Mizoue T, Noda m, Inoue M, Tsugane S; Japan Public Health Center-based Prospective Study Group.	Dietary patterns and type 2 diabetes in Japanese men and women: the Japan Public Health Center-based Prospective Study.	Eur J Clin Nutr.	67	18-24	2013
Okumura A, Suzuki T, Miyatake H, Okabe T, Hashimoto Y, Miyakawa T, Zheng H, Unoki-Kubota H, Ohno H, Dohmae N, Kaburagi y, Miyazaki Y, Tanokura	Leukocyte cell-derived chemotaxin 2 is a zinc-binding protein.	FEBS Let.	587	404-409	2013
Yokouchi H, Yasuda K, Takeda N, Kaburagi y, Yamamoto S.	Angiopoietin-like protein 4 (ANGPTL4) is induced by high glucose in RPE cells and exhibits potent angiogenic ac tivity on retinal endothelial cells.	Acta Ophthalmol	91	e289-297	2013

JOURNAL OF PROTEOMICS 84 (2013) 40–51

Available online at www.sciencedirect.com

SciVerse ScienceDirect

www.elsevier.com/locate/jprot

Differential proteome analysis of serum proteins associated with the development of type 2 diabetes mellitus in the KK-A^y mouse model using the iTRAQ technique

Eri Takahashi[a,b,1], *Akinori Okumura*[a,1], *Hiroyuki Unoki-Kubota*[a,1], *Hisashi Hirano*[b], *Masato Kasuga*[c], *Yasushi Kaburagi*[a,*]

[a]*Department of Diabetic Complications, Diabetes Research Center, Research Institute, National Center for Global Health and Medicine, Tokyo, Japan*
[b]*Graduate School of Nanobioscience, Yokohama City University, Yokohama, Japan*
[c]*National Center for Global Health and Medicine, Tokyo, Japan*

ARTICLE INFO

Article history:
Received 24 October 2012
Accepted 19 March 2013

Keywords:
Serum proteome
Type 2 diabetes mellitus
Quantitative mass spectrometry
Multiple reaction monitoring

ABSTRACT

To identify candidate serum molecules associated with the progression of type 2 diabetes mellitus (T2DM), we carried out differential proteomic analysis using the KK-A^y mouse, an animal model of T2DM with obesity. We employed an iTRAQ-based quantitative proteomic approach to analyze the proteomic changes in the sera collected from a pair of 4-week-old KK-A^y versus C57BL/6 mice. Among the 227 proteins identified, a total of 45 proteins were differentially expressed in KK-A^y versus C57BL/6 mice. We comparatively analyzed a series of the sera collected at 4 and 12 weeks of age from KK-A^y and C57BL/6 mice for the target protein using multiple reaction monitoring analysis, and identified 8 differentially expressed proteins between the sera of these mice at both time points. Among them, serine (or cysteine) peptidase inhibitor, clade A, member 3K (SERPINA3K) levels were elevated significantly in the sera of KK-A^y mice compared to C57BL/6 mice. An *in vitro* assay revealed that the human homologue SERPINA3 increased the transendothelial permeability of retinal microvascular endothelial cells, which may be involved in the pathogenesis of diabetes and/or diabetic retinopathy. With the identified proteins, our proteomics study could provide valuable clues for a better understanding of the underlying mechanisms associated with T2DM.

Biological significance

In this paper, we investigated the serum proteome of KK-A^y mice in a pre-diabetic state compared to that of wild type controls in an attempt to uncover early diagnostic markers of diabetes that are maintained through a diabetic phenotype. We used iTRAQ-based two-dimensional LC–MS/MS serum profiling, and identified several differentially expressed proteins at the pre-diabetic stage. The differential expression was confirmed by multiple reaction monitoring assay, which is fast gaining ground as a sensitive, specific, and cost-effective methodology for relative quantification of the candidate proteins. Using these techniques, we have identified eight candidate proteins of interest including SERPINA3K, which may be important in the pathology of T2DM and/or diabetic retinopathy.

* *Corresponding author at:* Department of Diabetic Complications, Diabetes Research Center, Research Institute, National Center for Global Health and Medicine, 1-21-1 Toyama, Shinjuku-ku, Tokyo 162-8655, Japan. Tel.: +81 3 3202 7181x2931; fax: +81 3 3202 7364.
E-mail address: kaburagi@ri.ncgm.go.jp (Y. Kaburagi).
[1] Contributed equally.

1874-3919/$ – see front matter © 2013 Elsevier B.V. All rights reserved.
http://dx.doi.org/10.1016/j.jprot.2013.03.014

1. Introduction

Diabetes mellitus is one of the most common metabolic disorders in the world, in which more than 90% of patients are diagnosed with type 2 diabetes mellitus (T2DM) [1]. The pathogenesis of T2DM is thought to be complicated, involving multiple genetic, metabolic, and environmental factors. Typically, it is characterized by hyperglycemia that is caused by defects in insulin secretion and its molecular action [2]. Initially, the effect of T2DM is limited to the detrimental loss of insulin-producing pancreatic β-cells. However, subsequent reduction in insulin secretion may lead to multiple malfunctions such as macrovascular complications including cardiovascular and cerebrovascular diseases, and microvascular complications including diabetic retinopathy and nephropathy [3].

Identifying individuals at high risk of T2DM prior to the clinical onset of the multiple malfunctions associated with T2DM is a major goal in diabetes research. Therefore, many efforts have been made to identify genetic and protein markers to reveal the molecular/cellular details or progression of diabetes [4–9]. Genome wide association studies have some clear advantages because genetic susceptibility, which does not change over time, can be identified at an early stage. While these markers provide a good foundation for the prediction and prevention of T2DM, the available tests are far from satisfactory due to their low-to-moderate sensitivity/specificity and/or late appearance in the disease process. As such, markers with increased specificity/sensitivity are urgently needed.

Proteomics has been used to identify novel disease markers that are differentially expressed during a pathological state in patients compared to healthy individuals. The systemic nature of T2DM indicates that the modulation of plasma proteins may be the cause or a consequence of the pathophysiology of this disease. To date, a few proteomic analyses of plasma related to T2DM have been reported [10–12]; however, analysis of the plasma proteomics of T2DM has been very limited and requires further investigations to find reliable diagnostic marker protein. Further, most previous serum proteomic analyses of T2DM have focused on the discovery of biomarkers, and have not stressed their potential to elucidate the pathophysiological mechanisms of the disease. Thus, the potential of serum proteomics to investigate the underlying disease mechanisms has been poorly addressed.

In this study, we analyzed the KK-A^y mouse model of T2DM in a pre-diabetic state. KK-A^y mice are obese, develop severe early-onset hyperinsulinemia, hyperglycemia, hypertriglyceridemia, and fatty liver, and are widely used as a model for T2DM [13]. We applied iTRAQ labeling coupled with offline 2-D LC–MS/MS proteomics technology to analyze quantitatively the protein expression profile of KK-A^y and C57BL/6 mice as well as to identify novel diagnostic marker proteins associated with the pathophysiological mechanisms of T2DM. To verify the candidate proteins that were differentially expressed among the two groups in the iTRAQ discovery study, we analyzed the time course changes of the candidate protein levels in the sera of KK-A^y and C57BL/6 mice using multiple reaction monitoring (MRM) analysis. We identified 8 proteins, including serine proteinase inhibitor A3K (SERPINA3K), that were expressed between the 2 groups. We further revealed that the human homologue SERPINA3 increased the permeability of retinal microvascular endothelial cells, which may be involved in the pathogenesis of diabetes and/or diabetic retinopathy.

2. Materials and methods

2.1. *Mouse sample collection*

KK-A^y/TaJcl (KK-A^y) and C57BL/6JJcl (C57BL/6) mice were purchased from Clea Japan Inc. (Tokyo, Japan). The mice were housed individually and fed standard mouse chow and water. At 4, 8, 12 and 16 weeks of age, body weights and fasting blood glucose levels were measured as described previously (n = 4/each group) [14]. Oral glucose tolerance test (OGTT) was performed on conscious mice after a 16 h fasting (n = 4/each group). The test was done by orally administrated glucose (2 mg per g body weight) and measurement of blood glucose at 15, 30, 45 and 60 min after loading. To perform proteomic analysis associated with the early onset of T2DM, we studied 4- and 12-week-old KK-A^y and C57BL/6 mice as a reference. Blood samples were obtained from retro-orbital venous plexus of the mice which had fasted over 16 h. The serum was immediately separated by centrifugation at 3000×*g* for 20 min at 4 °C, and was stored at −80 °C until analyzed. Animal care, use, and experimental protocols were approved by the local animal ethics committee of the National Center for Global Health and Medicine (approval ID: 12034) and performed in accordance with EU Directive 2010/63/EU.

2.2. *Protein depletion and purification*

For each group (C57BL/6 mice at 4 weeks, KK-A^y mice at 4 weeks, C57BL/6 mice at 12 weeks, and KK-A^y mice at 12 weeks), serum samples were prepared from the male mice. The seven most abundant proteins (albumin, IgG, α1-antitrypsin, IgM, transferrin, haptoglobin and fibrinogen) were depleted by using Seppro Mouse Spin Columns following the manufacturer's protocol (Sigma-Aldrich, St. Louis, MO, USA). The collected samples were desalted and concentrated using Amicon Ultra-4 3K (Millipore, Billerica, MA, USA). Protein concentration was determined using the Bradford protein assay (Bio-Rad Protein Assay; Bio-Rad Laboratories, Hercules, CA, USA).

2.3. *iTRAQ labeling*

An equal amount of depleted samples from each group was digested with MS-grade Trypsin Gold (Promega, Madison, WI, USA) and the peptides were labeled with iTRAQ reagents according to the manufacturer's instructions (iTRAQ Reagents 4-plex Applications Kit; AB Sciex, Framingham, MA, USA). Briefly, 25 μg of each depleted sample was reduced with 50 mM tris-(2-carboxyethyl)phosphine, alkylated with 84 mM iodoacetamide, and digested with Trypsin Gold at a protein-to-enzyme ratio of 10:1 at 37 °C overnight. For the analysis of serum protein expression in the KK-A^y mice, the tryptic digest samples prepared from the 3 KK-A^y mice were labeled with iTRAQ reagents (iTRAQ reporter ions of 115.1, 116.1 and 117.1 *m/z*). An equal amount of samples from the 3 KK-A^y mice and 3 C57BL/6 mice was pooled, labeled with

iTRAQ reporter ions of 114.1 m/z, and used as an internal standard (Supplementary Fig. 1). The sample set consisting of the 3 KK-A^y mice samples and an internal standard were combined and dried using a centrifugal concentrator (TOMY SEIKO CO., LTD., Tokyo, Japan) and dissolved in 100 μL of 10 mM ammonium formate, 25% ACN and 0.5% formic acid. For the analysis of serum protein expression in the C57BL/6 mice, the tryptic digest samples prepared from the 3 C57BL/6 mice were labeled with iTRAQ reagents (iTRAQ reporter ions of 115.1, 116.1 and 117.1 m/z). The sample set consisting of the 3 C57BL/6 mice samples and an internal standard were combined, dried, and dissolved in 10 mM ammonium formate, 25% ACN and 0.5% formic acid as well.

2.4. *Separation with strong cation exchange chromatography (SCX)*

Two iTRAQ labeled sample sets were fractionated separately using HPLC (Gilson Medical, Middleton, WI, USA) equipped with a model 305 LC pump, a UV/VIS-155detector, Rheodyne injection valve (model 7725) with 500 μL fixed loop injector, an FC203B autosampler, and a TSK gel SP-2SW column (4.6 mm I.D. × 250 mm cm, ϕ5 μm; TOSOH, Tokyo, Japan) (Supplementary Fig. 1). The mobile phase consisted of (A); 10 mM ammonium formate and 25% ACN, pH 3.0 and (B); 500 mM ammonium formate and 25% ACN, pH 6.8. The mixed iTRAQ labeled samples were dissolved in 100 μL of buffer A and separated at a flow rate of 0.6 mL/min using a 2-step liner gradient; 0% B for 10 min, 0–30% B for 40 min, 30%–100% for 10 min, and 100% B for 10 min. A total of 18 fractions were collected, dried using the centrifugal concentrator, dissolved in 2% ACN and 0.1% TFA, and desalted with MonoSpin C18 (GL Science, Tokyo, Japan).

2.5. *NanoLC–MS/MS*

Fractionated samples prepared from each iTRAQ labeled sample set were analyzed by LC–MS/MS (Supplementary Fig. 1). NanoLC–MS/MS system was conducted by a QSTAR ELITE Q-TOF mass spectrometry (AB Sciex) equipped with a nano-electro-spray ionization source, a nanoLC system (Paradigm MS4; Michrom Bioresources, Auburn, CA, USA), and an HTC-PAL autosampler (CTC Analytics, Zwingen, Switzerland). The SCX-fractionated peptides dissolved in 2% ACN and 0.1% TFA were loaded onto a trap column (0.3 × 5 mm, L-Column ODS; Chemicals Evaluation and Research Institute, Tokyo, Japan), and separated by RP capillary LC (L-Column Micro; Chemicals Evaluation and Research Institute) at a flow rate of 300 nL/min. The eluent gradient consisted of 95% buffer A (2% ACN and 0.1% TFA) to 45% buffer B (90% ACN and 0.1% TFA) for 120 min. A spray voltage of 1800 V was applied.

2.6. *Data analysis of iTRAQ experiments*

Peptide and protein identification was performed through automated database searching using the Mascot search engine (version 2.4.0; Matrix Science, London, UK). All tandem mass spectra were searched for species of *Mus musculus* against the UniProtKB/Swiss-Prot database containing 536,489 sequence entries (release—2012_06). Carbamidomethylation of cysteine and iTRAQ reagents (N-terminus and Lysine side chain) were chosen as the fixed modifications, and oxidation of methionine and iTRAQ reagents (Tyrosine) were searched as the variable modifications. Searches were performed with trypsin cleavage specificity allowing 1 missed cleavage; mass tolerance for monoisotopic peptide identification was set to ±0.1 Da and ±0.1 Da for fragment ions. The instrument setting was "ESI-QUAD-TOF". For the relative quantification of each peptide, the ratio of the areas under the signature peaks of 115, 116, 117, and 114 Da (as an internal standard), which are the masses of the tags that correspond to the iTRAQ reagents, was used. Data file processing and relative quantification were performed using ProteinPilot 3.0 software (AB Sciex) and the Paragon algorithm. The search parameters used were: iTRAQ 4-plex (peptide labeled), carbamidomethylation of cysteine, and UniProtKB/Swiss-Prot database for *M. musculus*. The confidence threshold for protein identification was an unused ProtScore >1.3 (95% confidence interval). Protein quantification required at least one unique peptide, and relative protein quantitation value normalized to an internal standard for each sample was used for the statistical analysis.

2.7. *Protein networks and functional analysis*

Differentially expressed serum proteins between the KK-A^y and C57BL/6 mice were subjected to functional pathway analysis using Ingenuity Pathway Analysis (IPA) (Ingenuity Systems, available at www.ingenuity.com). Protein analysis was performed through Database for Annotation, Visualization and Integrated Discovery (DAVID) version 6.7 (available at http://david.abcc.ncifcrf.gov/home.jsp) [15].

2.8. *Multiple reaction monitoring (MRM) analysis*

For making transitions for each peptide in MRM, MRMPilot software version 2.0 (AB Sciex) was used. High-confidence peptides with a rich product ion spectrum for each target protein were selected for relative quantification analysis using MRM. Peptides that had modifications, such as partially oxidized methionine, were avoided and when possible, two peptides were used per protein. MRM run was performed using a 5500 QTRAP hybrid triple quadrupole/linear ion trap mass spectrometer (AB Sciex) coupled with a Paradigm MS4 nanoLC system in the MRM mode. Test runs of the synthetic peptides mixture were performed to establish the retention time window (±5 min) for each peptide ion. During the test run, full scan MS/MS acquisitions (EPI, Enhanced Product Ion) were also triggered when MRM signal exceeded 1000 counts, with a mass tolerance of 250 mDa, the Linear Ion Trap (LIT) was set at 5 ms fixed fill time. Samples were separated on a C18 column (L-Column Micro, L-Column ODS; Chemicals Evaluation and Research Institute) with solvent A (2% ACN and 0.1% formic acid) and solvent B (90% ACN and 0.1% formic acid). The flow rate was set to 300 nL/min at room temperature, after which linear gradient elution was performed by increasing the mobile phase composition from 5 to 40% solvent B over 90 min. The gradient was then ramped to 95% B for 10 min and 5% B for 10 min to equilibrate the column for the next run. The total LC running time was 110 min. A 5500 QTRAP mass spectrometer was interfaced with a nanospray

source. The ionspray voltage was set to 2300 V. The source temperature was set to 150 °C. The curtain gas, collision gas, and ion source gas 1 were 10, 12, and 15, respectively. The declustering potential, entrance potential, and collision cell exit potential were set to 70 V, 10 V, and 15 V, respectively. Unit resolutions were used at quadrupole part 1 and quadrupole part 3. The collision energy for each transition was calculated by MRMPilot software version 2.0. In the MRM runs, the target scan time was set to 2 s. Five hundred ng of mouse serum sample was digested with mass spectrometry grade Trypsin Gold and Lysyl Endopeptidase (Wako Pure Chemicals, Osaka, Japan) for MRM analysis. The digested sample was transferred to a new tube and 10 fmol of human CUB domain containing protein 1 peptide (EEGVFTVTPDTK) was also added to each sample as an internal standard. Samples were analyzed by LC–MRM on the 5500 QTRAP using the predetermined MRM method. Data were processed using the MultiQuant program (version 2.0; AB Sciex). The most intense peak of the transition was used for quantitation. The area under the most intense peak was calculated, and normalized to the input internal standard. The peak of the transition for the input internal standard was also used for the quality control measure. Duplicate analyses were performed for each of the mouse serum samples.

2.9. Cell culture

Primary human retinal microvascular endothelial cells (HRMVECs) were purchased from the Applied Cell Biology Research Institute (Kirkland, WA, USA). HRMVECs were cultured on type I collagen-coated cell culture dishes in EGM-2 MV medium (EBM-2 supplemented with EGM-2 MV SingleQuots; Lonza, Walkersville, MD, USA). The cells were used at passages 7–9.

2.10. Expression and purification of recombinant human SERPINA3 protein

Human *SERPINA3* cDNA excluding signal sequences was amplified from human liver mRNA (Clontech, Palo Alto, CA, USA) by RT-PCR and cloned into the expression vector pET-21a(+) (Merck KGaA, Darmstadt, Germany). The C-terminal histidine-tagged SERPINA3 protein was expressed in *Escherichia coli* BL21 (DE3) cells and purified by Ni-NTA affinity chromatography, as described previously [16]. The protein was passed through a polymyxin B affinity column (Detoxi-gel Endotoxin Removing Columns; Thermo Scientific, Rockford, IL, USA) to remove contaminating endotoxins. The eluted SERPINA3 protein was concentrated with a membrane filter (Amicon Ultra-15 3K; Millipore) and stored at −80 °C until use.

2.11. Electric cell substrate impedance sensing (ECIS) assays

Transendothelial electrical impedance was measured using an ECIS Zθ instrument (Applied Biophysics, Troy, NY, USA). HRMVECs were plated at confluence in 8W10E+ (for barrier functional measurement) or 8W1E (for wound-healing assay) gold electrode culture plates (Applied Biophysics) precoated with type I collagen. The cells were cultured in EGM-2 MV medium for 16 h, after which the medium was changed to EBM-2 medium supplemented with 0.5% FBS (Lonza). For barrier functional measurement, HRMVECs were incubated with SERPINA3 protein at a final concentration ranging from 100 to 500 μg/mL and the incubation was continued for a further 40 h. Multi-frequency measurements (11 frequencies at 0.0625, 0.125, 0.25, 0.5, 1, 2, 4, 8, 16, 32, and 64 kHz) were taken for each of the 16 wells at a fixed interval of 180 s. To better characterize the divergent changes in barrier function caused by SERPINA3 in HRMVECs, we applied the model of Giaever and Keese [17] to resolve our ECIS data into three components: Rb (cell-to-cell resistances), α (cell-to-extracellular matrix interaction), and Cm (membrane capacitance). For the wound-healing assays, serum-starved confluent cells treated with SERPINA3 at a final concentration ranging from 100 to 500 μg/mL for 6 h were submitted to an elevated voltage pulse of 60 kHz frequency, 1400 μA amplitude, and 20 s duration, which killed and removed cells from the electrode. The kinetics of wound closure over the electrode were then assessed by continuous impedance measurements at 16 kHz for 24 h. HRMVECs incubated without SERPINA3 were used as a control.

2.12. Cell proliferation analysis by 5-bromo-2′-deoxyuridine (BrdU) incorporation

HRMVECs (1.0×10^4 cells/well) were seeded in type I collagen-coated 96 well plates with EGM2 MV medium for 16 h and incubated with EBM2 medium supplemented with 0.5% FBS for another 8 h. The cells were treated with SERPINA3 protein for 18 h, after which BrdU labeling solution was added and incubated for another 6 h. The proliferation rate was measured using cell proliferation ELISA, BrdU chemiluminescence kit (Roche Applied Science, Mannheim, Germany) according to the manufacturer's protocol.

2.13. Data analysis and statistics

The distributions of continuous data were tested for normality by the Shapiro–Wilk test. Values were presented as mean ± SD for normally distributed values. Differences between the groups were tested using Student's two-sided *t*-test or a two-tailed Mann–Whitney *U* test, as appropriate. All calculations were performed with Microsoft Excel 2010 or the SPSS software version 20 (IBM, Armonk, NY, USA). The differences were considered statistically significant for p values smaller than 0.05.

3. Results

3.1. Comparative analysis of the serum proteomic changes in the paired KK-A^y versus C57BL/6 mice

Characteristics of KK-A^y mice are shown in Fig. 1. KK-A^y mice were originally developed by Nishimura by crossing the KK mouse with the A^y mouse (C57BL/6J-A^y) [18]. C57BL/6J mice are generally used as nondiabetic controls. Therefore, we used C57BL/6J mice as a control for KK-A^y. As KK-A^y mice grew older, body weight and glucose concentration were gradually increased as reported previously [14]. Body weights of KK-A^y mice were significantly increased from 4 to 16 weeks of age

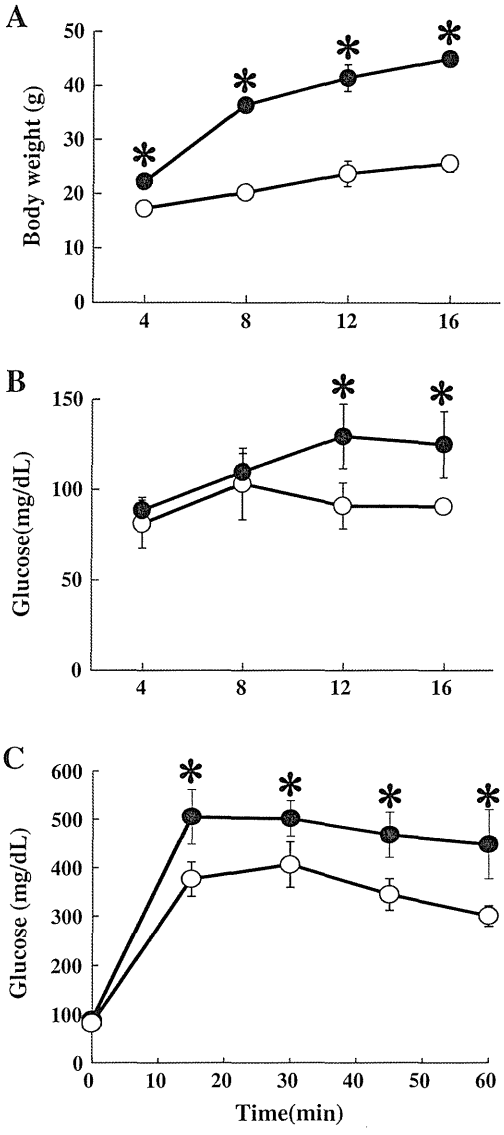

Fig. 1 – Characteristics of KK-A^y mice. Time course changes of body weight (A) and fasting blood glucose (B) in 4–16 weeks old KK-A^y (closed circles) and C57BL/6 mice (open circles). (C) Oral glucose tolerance test in 4-week-old KK-A^y and C57BL/6 mice. Plasma glucose levels at 15, 30, 45 and 60 min after oral glucose administration were measured. C57BL/6 mice are served as control. Each value represents mean ± SD (n = 4 for each group). *, $p < 0.05$ compared with the values of control.

compared to those of age-matched C57BL/6 mice (Fig. 1A) and the glucose concentrations were significantly elevated in 12- and 16-week-old KK-A^y mice compared with those of age-matched C57BL/6 mice (Fig. 1B). OGTT was analyzed at 4 weeks of age (Fig. 1C). The glucose concentrations during the course of glucose loading were significantly higher in 4-week-old KK-A^y mice than in C57BL/6 mice. This result indicates that glucose intolerance was initiated in 4-week-old KK-A^y mice although the fasting glucose concentrations did not show any differences between the 4-week-old KK-A^y mice and C57BL/6 mice. To obtain insights into the molecular differences from the early onset of T2DM, we investigated differential serum proteome analysis between 4-week-old male KK-A^y as T2DM and age-matched male C57BL/6 mice as wild-type mice. In the 2-D LC–MS/MS analysis, a total of 227 unique proteins were identified in the iTRAQ experiments at both the significance threshold $p < 0.05$ and the 5% false discovery rate threshold level (Supplementary Table 1). For the selection of differentially expressed proteins, we selected proteins using the following criteria: (1) the protein quantitation values between the KK-A^y and C57BL/6 groups were significantly different with a p value <0.05. (2) Proteins detected only in one group were also included as differentially expressed proteins. A total of 45 proteins were selected as differentially expressed proteins. Twenty five proteins among the 45 proteins were found to be up-regulated (Tables 1 and 2), and the other 20 proteins were down-regulated (Tables 3 and 4).

3.2. *Interaction networks and functional pathway analysis*

To gain insights into the biological changes in the KK-A^y versus C57BL/6 mice, the differentially expressed proteins were categorized according to the Gene Ontology (GO) classes "cellular component" and "molecular function". In the cellular component of GO analysis, differentially expressed proteins were located in the extracellular space (64%), membrane attack complex (10%), high-density lipoprotein particle (13%), and plasma lipoprotein particle (13%) (Fig. 2A). According to the molecular functions, most of the differentially expressed proteins were associated with peptidase inhibitor activity (50%), serine hydrolase activity (31%), and lipoprotein binding (19%) (Fig. 2B).

In the IPA analysis, 45 differentially expressed proteins were eligible for network analysis based on the IPA Knowledge Base criteria. IPA generated 3 interaction networks (Supplementary Table 2). Top-rated networks are related to: metabolic disease, endocrine system disorders, and energy production (Fig. 3), and lipid metabolism, molecular transport, and small molecule biochemistry (data not shown). Each network consists of 35 proteins, of which 13 were included in our list, and had a score of 23. Fig. 3 shows that 7 of 13 differentially expressed proteins are modulated directly by peroxisome proliferator activated receptor α, Ppara (p-value of overlap = 3.75×10^{-9}, Supplementary Table 3). Furthermore, 3 of 14 differentially expressed proteins are shown to be modulated directly by nuclear factor, erythroid derived 2, like 2, Nfe2l2 (p-value of overlap = 3.73×10^{-2}, Supplementary Table 3), which also interacted with Ppara.

3.3. *Validation of the selected proteins by MRM analysis*

In the iTRAQ experiments, we analyzed 3 biological replicates per group. This small number of samples could introduce many false positive findings. For the validation of the iTRAQ results, we carried out relative quantification of the identified proteins by MRM analysis using an independent sample set (the sera obtained from 4-week-old KK-A^y and C57BL/6 mice (n = 5/each group)) from that used in the iTRAQ experiments. In this work, proteotyptic peptides were chosen based on iTRAQ results and shotgun proteomic identification data using MRMPilot software. For MRM, 34 of

Table 1 – Increased serum proteins in KK-A^y mice compared to C57BL/6 mice.

Accession number	Entry name	Protein name	Relative protein ratio [a]		KK-A^y: C57BL/6	p-Value
			KK-A^y	C57BL/6		
Q61147	CERU_MOUSE	Ceruloplasmin	1.29 ± 0.07	1.05 ± 0.04	1.23	1.2E−02
P42703	LIFR_MOUSE	Leukemia inhibitory factor receptor	1.05 ± 0.03	0.83 ± 0.09	1.27	3.3E−02
P11589	MUP2_MOUSE	Major urinary protein 2	1.02 ± 0.09	0.8 ± 0.03	1.27	2.9E−02
Q06890	CLUS_MOUSE	Clusterin	1.19 ± 0.06	0.93 ± 0.06	1.28	1.4E−02
P08226	APOE_MOUSE	Apolipoprotein E	1.25 ± 0.16	0.9 ± 0.07	1.38	4.9E−02
Q8K182	CO8A_MOUSE	Complement component C8 alpha chain	1.18 ± 0.03	0.74 ± 0.08	1.59	1.7E−03
P19221	THRB_MOUSE	Prothrombin	1.36 ± 0.05	0.85 ± 0.11	1.60	3.8E−03
P06683	CO9_MOUSE	Complement component C9	1.38 ± 0.12	0.81 ± 0.09	1.69	5.5E−03
P20918	PLMN_MOUSE	Plasminogen	1.03 ± 0.05	0.61 ± 0.04	1.70	9.9E−04
P02762	MUP6_MOUSE	Major urinary protein 6	1.73 ± 0.24	0.74 ± 0.12	2.34	6.6E−03
P07759	SPA3K_MOUSE	Serine protease inhibitor A3K	1.53 ± 0.12	0.60 ± 0.05	2.56	6.0E−04
P09813	APOA2_MOUSE	Apolipoprotein A-II	1.83 ± 0.45	0.64 ± 0.17	2.85	2.6E−02
P04186	CFAB_MOUSE	Complement factor B	1.58 ± 0.09	0.52 ± 0.09	3.05	3.1E−04

[a] The relative protein ratios to an internal standard identified by iTRAQ are used and expressed as mean ± SD.

45 differentially expressed proteins were selected by the criteria described in the Materials and methods. Forty eight peptides representing 34 proteins were selected for MRM analysis. Finally, a total of 102 transitions were used for targeting 34 peptides of 34 proteins. The complete transition list is shown in Supplementary Table 4. For each of the 34 target proteins, three transitions were monitored for each peptide. Supplementary Fig. 2 displays a typical XIC (extracted ion chromatogram) overlay of the predetermined different transitions for the 34 proteins. The XIC peaks of the different transitions for each target protein were detected at the same retention time. Each resulting MRM peak was also examined by full scan MS/MS. The MS/MS spectrum for each MRM peak confirmed the sequence validation of the hypothesized peptide as shown in Supplementary Fig. 3. Individual serum samples were digested and analyzed in duplicate. Among them, 17 proteins showed significant differences between 4-week-old KK-A^y and C57BL/6 mice, which validated the iTRAQ results (Table 5). Retinol-binding protein 4 (RBP4) was found to be increased in 4-week-old KK-A^y mice compared with C57BL/6 mice in the MRM analysis although the expression of RBP4 was decreased in KK-A^y mice in the iTRAQ result. The inconsistency has arisen from the selection of the peptides for the quantitation in the iTRAQ experiments. Relative protein quantitation of RBP4 in C57BL/6 mice was calculated using 4 peptides in the iTRAQ experiments; however, only 2 of the 4 peptides were used for the quantitation in KK-A^y mice samples because other 2 peptides were miscleaved in KK-A^y mice samples. Taken together, we adopted the data obtained from the MRM analysis for the RBP4 protein quantitation. Furthermore, for further analyses of the candidate proteins, the levels of the 34 proteins in the sera of 12-week-old KK-A^y and C57BL/6 mice were also analyzed by MRM analysis because the glucose concentrations in KK-A^y mice were significantly elevated from the age of 12 weeks compared to the C57BL/6 group (Fig. 1B). Eight of the 34 proteins still showed significant differences between 12-week-old KK-A^y and C57BL/6 mice. Among the 8 proteins mentioned above, proteins with a significant increase included 7 proteins: apolipoprotein (apo) A-II, carboxypeptidase N catalytic chain, clusterin, inter-alpha-trypsin inhibitor heavy chain H3, RBP4, serine protease inhibitor A3K (SERPINA3K), and serum amyloid P-component; and another protein with a significant decrease was apo A–I (Table 5).

Table 2 – Identified and quantitated serum proteins only in KK-A^y mice.

Accession number	Entry name	Protein name	Relative protein ratio [a]
Q8BH35	CO8B_MOUSE	Complement component C8 beta chain	1.54 ± 0.10
Q8R121	ZPI_MOUSE	Protein Z-dependent protease inhibitor	1.21 ± 0.07
Q9ET66	PI16_MOUSE	Peptidase inhibitor 16	1.41 ± 0.15
Q9WVJ3	CBPQ_MOUSE	Carboxypeptidase Q	1.05 ± 0.04
Q9JJN5	CBPN_MOUSE	Carboxypeptidase N catalytic chain	1.01 ± 0.16
P31532	SAA4_MOUSE	Serum amyloid A-4 protein	1.43 ± 0.18
P00920	CAH2_MOUSE	Carbonic anhydrase 2	1.33 ± 0.15
P02535	K1C10_MOUSE	Keratin, type I cytoskeletal 10	1.72 ± 0.86
P12246	SAMP_MOUSE	Serum amyloid P-component	1.34 ± 0.20
P52480	KPYM_MOUSE	Pyruvate kinase isozymes M1/M2	1.14 ± 0.16
Q5FW60	MUP20_MOUSE	Major urinary protein 20	3.00 ± 0.75
Q61704	ITIH3_MOUSE	Inter-alpha-trypsin inhibitor heavy chain H3	1.14 ± 0.11

[a] The relative protein ratios to an internal standard identified by iTRAQ are used and expressed as mean ± SD.

3.4. *SERPINA3-induced changes in endothelial cell monolayer permeability*

Among the 8 differentially expressed proteins, SERPINA3K was chosen for further analyses. SERPINA3K was selected on the basis of the possible implications for diabetic retinopathy

Table 3 – Decreased serum proteins in KK-A^y mice compared to C57BL/6 mice.

Accession number	Entry name	Protein name	Relative protein ratio [a]		KK-A^y: C57BL/6	p-Value
			KK-A^y	C57BL/6		
Q00724	RET4_MOUSE	Retinol-binding protein 4	0.71 ± 0.06	1.40 ± 0.25	0.51	2.0E−02
P11859	ANGT_MOUSE	Angiotensinogen	0.73 ± 0.10	1.22 ± 0.19	0.60	3.1E−02
P23953	EST1C_MOUSE	Carboxylesterase 1C	0.62 ± 0.03	1.04 ± 0.06	0.60	9.6E−04
Q60994	ADIPO_MOUSE	Adiponectin	0.68 ± 0.08	1.09 ± 0.13	0.62	1.8E−02
P32261	ANT3_MOUSE	Antithrombin-III	0.75 ± 0.07	1.19 ± 0.05	0.63	1.5E−03
O08677	KNG1_MOUSE	Kininogen-1	0.61 ± 0.04	0.90 ± 0.10	0.67	1.7E−02
Q00623	APOA1_MOUSE	Apolipoprotein A-I	0.98 ± 0.01	1.42 ± 0.06	0.69	4.3E−04
P21614	VTDB_MOUSE	Vitamin D-binding protein	0.84 ± 0.03	1.18 ± 0.01	0.71	7.6E−05
Q8BND5	QSOX1_MOUSE	Sulfhydryl oxidase 1	0.80 ± 0.04	1.08 ± 0.04	0.74	2.9E−03
O89020	AFAM_MOUSE	Afamin	0.88 ± 0.05	1.18 ± 0.02	0.74	1.5E−03
Q61730	IL1AP_MOUSE	Interleukin-1 receptor accessory protein	0.63 ± 0.02	0.84 ± 0.06	0.74	9.8E−03
Q06770	CBG_MOUSE	Corticosteroid-binding globulin	1.38 ± 0.13	1.81 ± 0.12	0.76	2.7E−02
P26262	KLKB1_MOUSE	Plasma kallikrein	0.76 ± 0.07	0.98 ± 0.07	0.78	3.6E−02
Q91X72	HEMO_MOUSE	Hemopexin	0.79 ± 0.10	1.02 ± 0.06	0.78	4.9E−02
Q61129	CFAI_MOUSE	Complement factor I	0.82 ± 0.07	0.98 ± 0.04	0.84	4.4E−02
Q01339	APOH_MOUSE	Beta-2-glycoprotein 1	0.78 ± 0.04	0.91 ± 0.01	0.86	1.5E−02

[a] The relative protein ratios to an internal standard identified by iTRAQ are used and expressed as mean ± SD.

in rat models [19,20]. However, it remains to be elucidated whether human homologue, SERPINA3 is associated with the development of T2DM and/or diabetic retinopathy. Blood-retinal barrier breakdown contributes to macular edema, which occurs in over 25% of people with diabetes and correlated highly with visual impairment in people with diabetic retinopathy [21]. Therefore, we focused on the effects of SERPINA3 on endothelial cell monolayer permeability. To this end, we sought to investigate the impact of SERPINA3 on HRMVECs. Post-confluent serum-starved HRMVECs incubated with SERPINA3 exhibited a dose-dependent increase in endothelial permeability reflected as a decrease in transendothelial electrical resistance, whereas electrical impedance for the untreated HRMVECs was almost unchanged. Fig. 4A is a representative ECIS graph demonstrating the real-time loss of electrical resistance across the HRMVEC monolayer. Permeability increased steadily after SERPINA3 was added, and continued to decline up to 8 h after treatment. Fig. 4B–D is the typical real-time traces of the Rb, α, and Cm in the SERPINA3-treated HRMVECs. After HRMVECs were treated with SERPINA3 (time = 0 in Fig. 4B–D), the cell-to-cell resistances gradually decreased, and the cell-to-extracellular matrix interaction slightly decreased, whereas membrane capacitance was almost unchanged. These results indicate that SERPINA3 treatment mainly caused the decrease of HRMVEC cell-to-cell resistances. Consistent with the ECIS data, we observed that SERPINA3 treatment caused a massive disruption of HRMVEC monolayers (data not shown).

Table 4 – Identified and quantitated serum proteins only in C57BL/6 mice.

Accession number	Entry name	Protein name	Relative protein ratio [a]
P09581	CSF1R_MOUSE	Macrophage colony-stimulating factor 1 receptor	1.23 ± 0.07
Q62351	TFR1_MOUSE	Transferrin receptor protein 1	1.34 ± 0.36
Q8CIF4	BTD_MOUSE	Biotinidase	1.10 ± 0.13
P04939	MUP3_MOUSE	Major urinary protein 3	1.99 ± 0.49

[a] The relative protein ratios to an internal standard identified by iTRAQ are used and expressed as mean ± SD.

3.5. *SERPINA3-induced changes in endothelial cell proliferation and migration*

Proliferation and migratory capability of vascular endothelial cells have a pivotal role in the maintenance of microvascular integrity and angiogenesis. Proliferative capacity of HRMVECs treated with or without SERPINA3 was compared. We found that treatment with SERPINA3 barely affected the proliferative ability in HRMVECs (Fig. 5A).

To assess the effects of SERPINA3 on migratory capability of HRMVECs, an ECIS-based wound-healing assay was performed. We conducted a wounding experiment on single-point ECIS arrays with a single 250 μm-diameter working electrode from which the interrogating electrical current originates, then passes through the monolayer and finally reaches the surrounding counterelectrode. Again, monolayers were found to mature when measured electrically. Post-confluent serum-starved HRMVECs were treated with various doses of SERPINA3 for 6 h, and then monolayers were electrically removed from the central working electrode by driving 1400 μA at 60 kHz through the circuit for 20 s. When assessed 18 h after the SERPINA3 treatment, little differences were observed between the four conditions (Fig. 5B). After completion of the wound closure process, monolayer resistance was found to return to values similar to prewounding levels.

4. Discussion and conclusions

In this paper, we investigated the serum proteome of KK-A^y mice in a pre-diabetic state compared to wild C57BL/6 mice in an attempt to uncover early diagnostic markers of diabetes

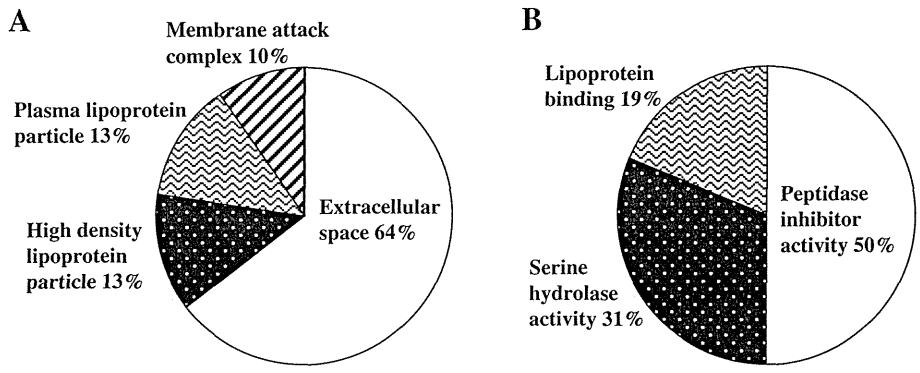

Fig. 2 – Gene ontology terms for cellular components (A), and molecular functions (B) of the differentially expressed proteins between the sera of KK-A^y and C57BL/6 mice.

that are maintained through a diabetic phenotype. We used iTRAQ-based two-dimensional LC–MS/MS serum profiling, and identified several differentially proteins at the pre-diabetic stage. The differential expression was confirmed by MRM analysis, which is fast gaining ground as a sensitive, specific, and cost-effective methodology for relative quantification of candidate proteins. Using these techniques, we have identified eight candidate proteins of interest including SERPINA3K, which may be important in the pathology of T2DM and/or diabetic retinopathy.

Several published studies have reported proteomic alterations in diabetes. During the preparation of this manuscript, Ressom et al. reported a similar approach for a large scale proteomic study aimed at identifying and validating changes

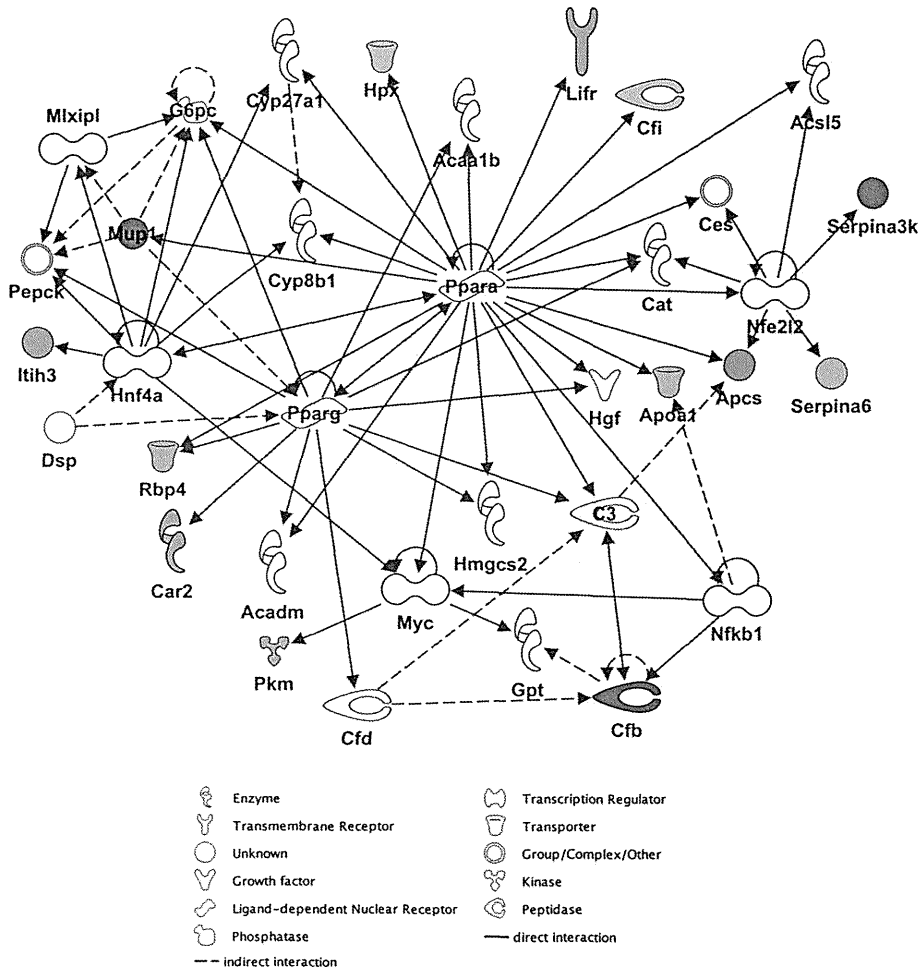

Fig. 3 – Interaction network analysis based on the IPA Knowledge Base criteria. The top-rated network is shown. This network is related to metabolic disease, endocrine system disorders, and energy production. Colored molecules: green; decreased in KK-A^y mice sera, and red; increased in KK-A^y mice sera.